

Modeling of rain drop size distribution for a tropical hot semi-arid site in India

B S Jassal^{1,§,*}, Anurag Vidyarthi^{1,#}, R Gowri^{1,%} & Ashish K Shukla^{2,~}

¹Department of Electronics & Communication Engineering, Graphic Era University, Dehradun 248 002

²Space Applications Centre, Ahmedabad 380 015

E-mail: [§]bsjassal@yahoo.co.in, [#]vidyarthianurag@yahoo.co.in, [%]ravigowri07@gmail.com, [~]ashishs@sac.isro.gov.in

Received 24 March 2011; revised 30 September 2011; accepted 12 October 2011

Data on rain drop size distribution, collected at Ahmedabad, India, has been analysed to develop empirical model on drop size distribution (DSD). Out of the various DSD models available in literature, analysis has been done for lognormal distribution as it has been reported to be suitable for tropical regions. The empirical model has been derived on the basis of fit parameters evaluated from experimental data. It is observed that data fits well in lognormal distribution for Ahmedabad.

Keywords: Empirical model, Rain drop size distribution (DSD), Rain induced attenuation, Lognormal distribution

PACS No.: 92.40.eg

1 Introduction

The demand for allocation towards higher end of electromagnetic spectrum, especially above 10 GHz, is increasing day by day to meet the demand of higher data rate for various communication and multimedia requirements. Unfortunately, signal impairment due to rain is the most important factor at millimeter wave frequencies (above 10 GHz) and is the limiting factor in satellite/terrestrial link design, especially for tropical and equatorial regions which experience very heavy rainfall. The rainfall can cause several decibels of attenuation resulting into a long outage time, thus, affecting reliability of communication link. It is, therefore, necessary to have accurate estimation of rain induced attenuation. Several methods have been reported¹. Measurement of sky noise temperature during clear weather and rainy conditions by radiometer is one way to determine the attenuation due to rain. But due to limited dynamic range of the radiometer, it does not predict attenuation accurately at high rain rates. Signal strength measurement by monitoring satellite beacon signals is another widely used method for estimating rain attenuations. A lot of attenuation measurements have been done using Advanced Communications Technology Satellite (ACTS), Olympus satellites at 30/20 GHz (ref. 2). However, in the absence of hardware needed to do measurements by means of radiometer or beacon, the method generally used is to estimate the rain induced

attenuation from the knowledge of the rain drop size distribution (DSD). Therefore, worldwide measurements have been carried out on DSD using disdrometer³⁻⁶. From the various studies done on DSD, it is now well established that the distribution of the drop sizes falling at particular rain intensity varies from place to place depending on meteorological conditions and so, is the attenuation at a particular frequency.

Modeling of the rain drop size distribution (DSD) has been reported by many researches, viz. Marshall & Palmer⁷, Joss & Waldvogel⁸, Joss & Gori⁹, etc. Exponential DSD has been the most widely used analytical parameterization for the rain drop size distribution:

$$N(D) = N_0 e^{(-\lambda D)} \quad \dots (1)$$

where, $N(D)$, is the number of drops per unit volume per unit interval of drop diameter D . The parameters N_0 and λ can be determined experimentally. Marshall & Palmer suggested that $N_0 = 8000 \text{ m}^{-3} \text{ mm}^{-1}$ and $\lambda = 4.1R^{0.21} \text{ mm}^{-1}$, where, R , is the rainfall rate in mm h^{-1} .

Although this model is simple, it has not been found applicable in many of the subsequent measurements made on DSD, especially when sampling time is 1 min or less. It tends to exaggerate the number of smallest and largest drops⁹. Many researchers have preferred the two-parameter

exponential distribution, which does not restrict N_0 to any fixed value. Some researchers¹⁰⁻¹² have suggested the use of gamma distribution:

$$N(D) = N_0 D^\mu e^{-\lambda D} \quad \dots (2)$$

Deviations from the exponential model are expressed in terms of the curvature parameter μ . Equation (2) reduces to exponential model for $\mu = 0$.

For tropical countries, based on the data collected on rate of rain fall and DSD, most of the researchers¹³⁻¹⁵ have suggested the use of three parameter lognormal distribution:

$$N(D) = [N_T / (\sqrt{2\pi} \ln(\sigma) \cdot D)] \exp[-\ln^2(D/D_g)/(2\ln^2\sigma)] \quad \dots (3)$$

where, D_g , is the geometric mean of drop diameters; σ , represents the standard geometric deviation, which is a measure of the breadth of the spectrum; and N_T , the total number of drops m^{-3} .

Out of the various DSDs explained mathematically by exponential, gamma and lognormal distributions, the suitability of a particular type of model for a particular geographical area depends on the rain characteristics in that climatic zone. Variability of DSD for different climatic regions is a major concern for the tropical region¹⁶, which has huge diversity in climatic conditions. For example, in India, different meteorological regions like coastal areas, desert of Rajasthan, Himalayan mountains experience widely different amount of rainfall in terms of intensity and quantity.

Indian Space Research Organization (ISRO), as a part of earth-space propagation experiment over Indian region, conducted ground based measurements on rate of rainfall and drop size distribution at five different geographical locations, namely, Ahmedabad, Shillong, Thiruvananthapuram, Kharagpur and Hassan¹⁶. These locations fall in different climatic zones of India with different rain characteristics. Graphic Era University, Dehradun has been entrusted with the task of analysis of data for modeling DSD and rain attenuation. The present paper discusses the modeling of DSD for Ahmedabad from the data collected, in 2007, using impact type disdrometer RD-80. Subsequently, DSD model will be used for estimation of specific attenuation ($dB km^{-1}$) at different rain rates and frequencies based on calculation of Mie scattering coefficients and extinction cross section of water drops of different diameters¹⁷.

Ahmedabad is located (latitude 23.03°N, longitude 72.58°E) in western India at an elevation of 53 m. The city is almost flat except for the small hills of Thaltej-Jodhpur Tekra and is located in a sandy and dry area. It has a hot semi-arid climate except for rainy seasons. It experiences south-west monsoon which extends from June to October with medium to heavy showers. The average annual rainfall is about 932 mm which includes infrequent heavy torrential rains. The average temperature varies from 45°C in summer to 15°C in winter.

2 Data collection

A Joss-Waldvogel impact type disdrometer (RD-80) (Joss and Waldvogel, 1967), manufactured by M/s Distromet Ltd, Switzerland, has been used for data collection. This instrument is used worldwide for drop size measurements. Lakshmi *et al.*⁵ has discussed various parameters of disdrometer. It converts vertical mechanical moment of the drops into electric pulses. The sampling area of the outdoor unit measures 50 cm^2 and the indoor unit consists of an analyzer ADA-90. The pulses are converted to 8-bit numbers. Thus, the disdrometer can measure 127 drop sizes which are subdivided into 20 drop size classes, all with differing diameter interval ΔD and diameters ranging from threshold value of 0.313 mm to 5.145 mm. The fall velocities of the drops with diameter corresponding to each drop class, ΔD , have been taken as suggested by Gunn & Kinzer¹⁸. The measurements of DSDs were taken with a temporal variation of 30 seconds for better resolution of rain rates. The disdrometer was installed at the roof top of a building (5 m high) to minimize the known sources of error like acoustic noises¹⁶. The location of Space Applications Centre (SAC) is such that the area is free from any industrial or acoustic noise

The disdrometer has certain limitations as far as counting the smaller and larger drops are concerned. The instrument has self noise control mechanism. When the ambient noise is high, there is possibility of error in the count of smaller drops. During high rain rate, a noise suppression circuit is activated which results in a reduction in the smaller drop count. Underestimation, at very heavy rain rate, can also be due to the finite time required by the instrument to recover from a drop strike and be ready for the next drop. This error is called dead time error and is corrected by using the correction matrix supplied by the manufacturer. But the effects of these smaller

drops are less on rain attenuation and are within 5% error limit¹⁹. Drops collected in all drop size classes of the disdrometer have been considered in the present analysis. It has much less effect on the DSD spectrum except at very low rain rates. In the present analysis, dead time correction is not considered. Possibility of error is due to accumulation of water on the sensor head which may change the calibration of the sensor. Generally, care is taken in mounting the sensor such that effects of acoustic noise and wind are minimized.

Data on rate of rainfall was also collected by a collocated tipping bucket rain gauge. The comparison of rain data has been reported²⁰. A correlation coefficient of 0.96 has been reported between the two data sets. Rain intensity (mm h^{-1}) estimated from disdrometer is more than that estimated from tipping bucket.

2.1 Data set

Some of the important parameters of the data set are given in Fig. 1. The total accumulated rainfall, as derived from DSD data, over the year has occurred for 9585 minutes. The monthly rainfall data shows that maximum rainfall (worst month) has occurred in the month of August which is for 5303 minutes. The rainfall data has also been grouped into number of monthly rain events with more than 5 mm accumulated rainfall and having more than two hour gap. The maximum number of events recorded was 13 in the month of August. The longest event recorded (1045 minutes) was also in the month of August and was also with highest rainfall of around 53 mm. Breakup of the event in terms of rain intensity (mm h^{-1}) and duration is given in Fig. 2. This analysis will be useful in the calculation of total outage time, an important parameter for communication engineer.

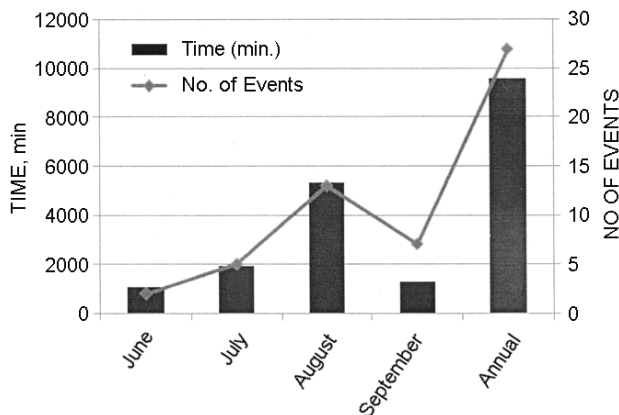


Fig. 1 — Statistics of rain fall events at Ahmedabad (2007)

3 Data analysis

3.1 Averaging the DSD

To obtain significant estimation of the parameters describing the DSDs, the instantaneous DSDs were averaged on monthly and annual basis in order to eliminate randomly varying components and to obtain stable distributions. The instantaneous DSDs of each sample were gathered in fourteen rain classes as shown in Table 1. Many researches^{14,15} have suggested exponential increase in the width of the rain classes because the rainfall duration is maximum at the low rain rates and decreases exponentially with increasing rain rate. The minimum and maximum rain rates are taken as less than 0.005 and 100 mm h^{-1} , respectively. Tokay & Short¹⁹ has categorized rain as very light (less than 1 mm h^{-1}), light (1 - 2 mm h^{-1}), moderate (2 - 5 mm h^{-1}), heavy (5 - 10 mm h^{-1}), very heavy (10 - 20 mm h^{-1}) and extreme (more than 20 mm h^{-1}) for classification of precipitation regimes, convective and stratiform, based on drop size distribution data collected with RD-69 disdrometer. However, in the present analysis, the limits are taken as 1 mm h^{-1} and 140 mm h^{-1} and divided into 14 ranges of 10 mm h^{-1} duration each. This is because it is the higher rain rate occurring for say 0.01% of the time which is of interest to communication engineer for rain induced fade margin calculations. The averaged DSDs were derived on monthly (June, July, August, September and October) and annual basis.

3.2 Data formatting and Analysis

First, the data were arranged in the ascending order of rain rate and then grouped according to rain rate classes as mentioned in Table 1. For every rain rate range, the average number of drops falling in each of the 20 drop size classes ($n_1, n_2, n_3, \dots, n_{20}$) were calculated. The drop number data, thus, arrived at was converted into number of drops per m^3 per mm in each drop size class²¹ using the relation:

$$N(D_i) = 10^4 [n_i / (ATv_i \Delta D_i)] \quad \dots (4)$$

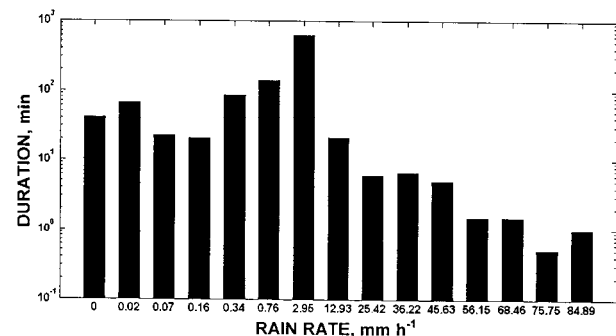


Fig. 2 — Analysis of heaviest rain events held on 08 August 2007

Table 1 — Parameters of averaged DSD for the year 2007

Rain rate bin	Class of rain rate, mm hr ⁻¹	No of DSDs	Avg rain rate, mm hr ⁻¹	N _T , m ⁻³	ln D _g	ln σ
1	1 ≤ R < 10	5795	3.12	263	-0.16215	0.382896
2	10 ≤ R < 20	655	14.01	548	0.035134	0.416028
3	20 ≤ R < 30	281	24.69	601	0.138219	0.440619
4	30 ≤ R < 40	191	34.90	652	0.212823	0.438949
5	40 ≤ R < 50	151	44.55	733	0.26083	0.430602
6	50 ≤ R < 60	98	54.33	812	0.30352	0.41536
7	60 ≤ R < 70	77	64.74	794	0.364191	0.410914
8	70 ≤ R < 80	44	74.66	979	0.380018	0.385726
9	80 ≤ R < 90	28	84.29	953	0.409113	0.384254
10	90 ≤ R < 100	16	95.20	684	0.492947	0.40856
11	100 ≤ R < 110	11	104.40	1054	0.481283	0.355569
12	110 ≤ R < 120	7	114.73	1038	0.508201	0.363597
13	120 ≤ R < 130	7	125.59	1291	0.497185	0.347714
14	130 ≤ R < 140	1	136.95	1151	0.546095	0.351404

where, $N(D_i)$, is the number of rain drops per unit volume per unit diameter interval, with average diameter D_i ; A , the surface area of sensor (50 cm² in present case); T , the sample time interval (0.5 min.); v_i , the terminal velocity of the rain drops with diameter D_i , as mentioned in Table 1; and ΔD_i , the channel width of the disdrometer with diameter D_i . The number of drops m⁻³ (N_i) in each drop diameter class, which is equal to $N(D_i) \times \Delta D_i$ were also calculated at each rain rate for calculating N_T , the total no of drops m⁻³. N_T is the sum of N_i values for the twenty drop diameter interval classes at each rain rate.

4 Modeling of DSD

4.1 Comparison between Lognormal and Gamma distribution

The distribution of experimental $N(D_i)$ values as arrived above, on annual basis, were analysed by fitting lognormal and gamma distributions using Table Curve software. The Table Curve software uses linear fitting procedure based on Fast Std option where in higher order polynomials and rationals are fitted by Gaussian elimination method.

The correlation coefficients obtained at different rain rates have been plotted in Fig. 3. The comparison shows that the values of correlation coefficients are better in case of lognormal distribution than those with gamma distribution. At most of the rain rates, the values are better than 0.95 in case of lognormal distribution. At the rain rate exceeding 0.01% of the time, which is around 76 mm h⁻¹ in the present case and is of interest for designing communication link, the value is almost reaching one. Hence, further analysis presented is based on lognormal distribution.

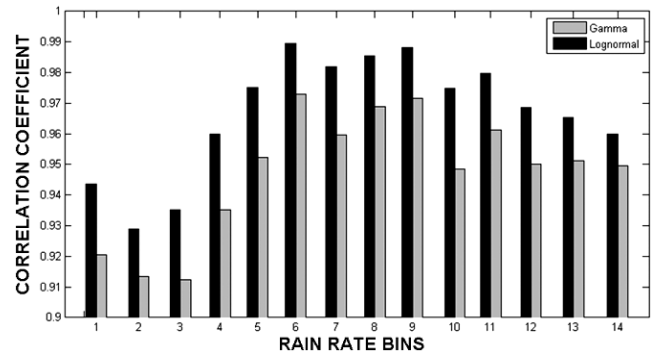


Fig. 3 — Comparisons of correlation coefficients of best fit lognormal and gamma distributions obtained for annual DSD data collected at Ahmedabad (2007)

4.2 Distribution based on experimentally derived fit parameters

The year 2007 contains disdrometer data for the period June - October 2007. Due to scanty rainfall data in the month of October, the same has not been analyzed as it will not affect the overall determination of DSD characteristics. The fit parameters of the lognormal distribution have been derived as explained below:

Parameters of the lognormal distribution [Eq. (3)] can be deduced, as per their definitions, from the disdrometer data by using following relations¹³:

$$\ln D_g = (1/N_T) \sum_{i=1}^{20} N_i \ln D_i \quad \dots (5)$$

$$\ln^2 \sigma = (1/N_T) \sum_{i=1}^{20} N_i (\ln D_i - \ln D_g)^2 \quad \dots (6)$$

where, N_T , is the number concentration (m⁻³) in the observed spectrum; and N_i , the number of drops in size category D_i .

Expression for lognormal distribution [Eq. (3)] is reproduced as:

$$N(D) = (\exp A/D) \exp\{-0.5[(\ln D - B)/C]^2\} \quad \dots (7)$$

where,

$$A = \ln[N_T/\sqrt{(2\pi)\ln\sigma}] \quad \dots (8)$$

$$B = \ln D_g \quad \dots (9)$$

$$C = \ln\sigma \quad \dots (10)$$

A, B and C in Eqs (8-10) are fit parameters of the lognormal distribution.

The values of geometric mean of drop diameters ($\ln D_g$) and standard deviation of drop diameters ($\ln\sigma$) were calculated using Eqs (5 and 6) on monthly and annual basis at each rain rate. The value of N_T , $\ln D_g$ and $\ln\sigma$ for annual distribution are also given in Table 1. The values of fit parameters A, B, and C of lognormal distribution were evaluated using Eqs (8), (9) and (10), respectively.

4.2.1 Monthly DSD analysis

The values of fit parameter A, B and C were evaluated for the month of June, July, August and September 2007 from the experimental DSD data for average rain rate corresponding to each rain rate bin. The monthly best fit curves, between $N(D_i)$ and drop diameter D_i , at each rain rate, using the fit parameters, were drawn using MATLAB software. The curves at a few selected rain rates, for the sake of clarity, are shown in Fig. 4. The experimental data points are plotted therein. The curves have been drawn for the average rain rates lying between 1 and 100 mm h⁻¹. It is seen from the curves that as the rain rate increases, the number of drops with different diameters also increase and at the same time, the mode of the distribution shifts towards higher drop diameter. The diameter of the largest falling drop also increases with increase in rain rate. The DSD curve at lower rain rate (14.01 mm h⁻¹) in the month of September shows different behaviour when compared with the curves at similar rain rates for other months. This finding needs to be analysed further as no definite explanation could be found at this moment.

4.2.2 Annual DSD analysis

The annual drop size distribution curves at different rain rates, as derived from experimental fit parameters A, B and C along with experimental data points are shown in Fig. 5. The behaviour of annual distribution curves is same as in monthly distribution curves.

4.3 Variability of annual fit parameters with number of samples

The values of fit parameters A, B and C for lognormal distribution were also evaluated for 30 sec (one disdrometer data sample), 1 min (two disdrometer data samples) and 5 min (ten disdrometer data samples) for each rain rate bins and compared with annual values as shown by histograms in Fig. 6. The histograms have been plotted at rain rates 24.69, 54.33, 74.66 and 95.20 mm h⁻¹, thus, covering almost the whole spectrum of rainfall. Not much variation in A parameter has been noticed with the change in

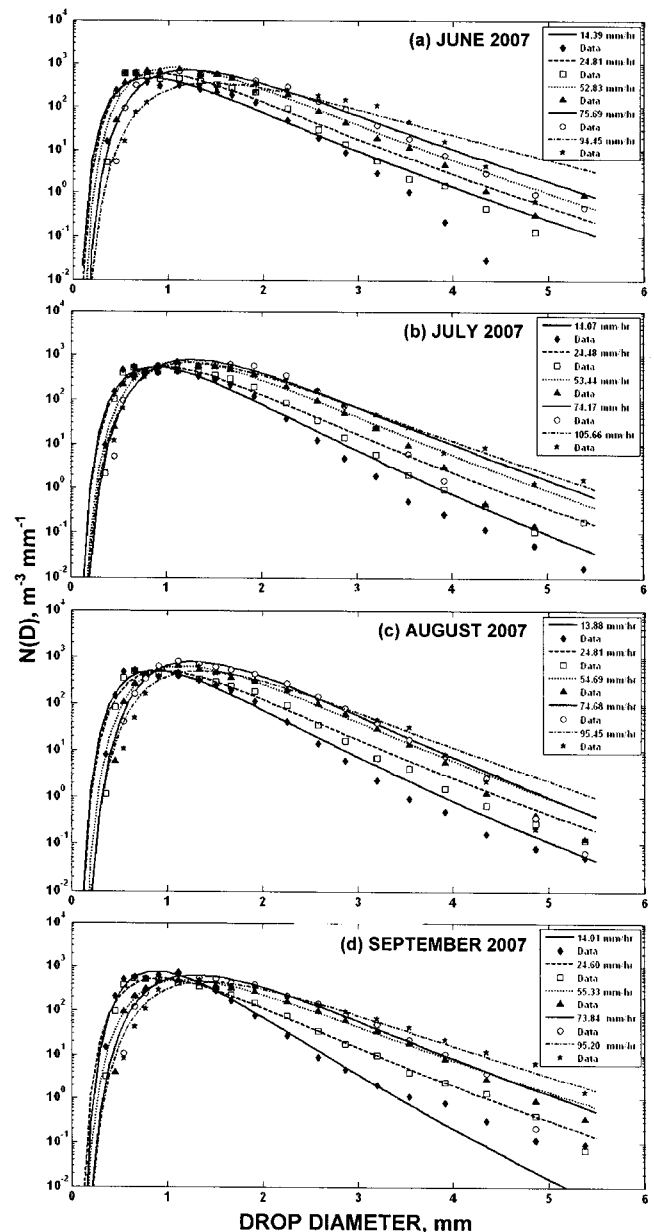


Fig. 4 — Rain drop size distribution spectrum for: (a) June 2007; (b) July 2007; (c) August 2007; and (d) September 2007

number of samples. In parameter B, though variability with number of samples is visible but no definite trend can be predicted. Parameter C is almost constant at 0.4 irrespective of number of samples and rain rate.

4.4 Modeling of annual fit parameters

The values of fit parameters A, B and C for annual drop size distribution, at each rain rate, have been plotted in Fig. 7. The values of fit parameters A, and B are found to vary almost linearly with exponential increase in rain rate at rain rate higher than 10 mm h^{-1} , whereas the parameter C is almost constant at value 0.4 at all rain rates. This finding about the fit parameter C has also been reported by Hari Kumar *et al.*¹⁴. The variation of fit parameters A, B and C with rain rate has been studied using the Table Curve software. The best fit equations have been found as:

$$A = A_0 + A_1(\ln R)^2 \quad \dots (11)$$

$$B = B_0 + B_1(\ln R)^2 \quad \dots (12)$$

$$C = \text{constant (0.4)} \quad \dots (13)$$

where, the coefficients A_0 , A_1 , B_0 , and B_1 are the fit parameters; and R , is the rain rate. Insertion of Eqs (11-13) in Eq. (3) gives the required empirical model for DSD. The values of coefficients A_0 , A_1 , B_0 , and B_1 , their correlation coefficients and fit standard error are given as under:

* Fit parameter	A	B
* Coefficients	$A_0: 5.561, A_1: 0.063$	$B_0: -0.183, B_1: 0.031$
* Correlation coefficient	0.883	0.992
*Fit Std error	0.160	0.018

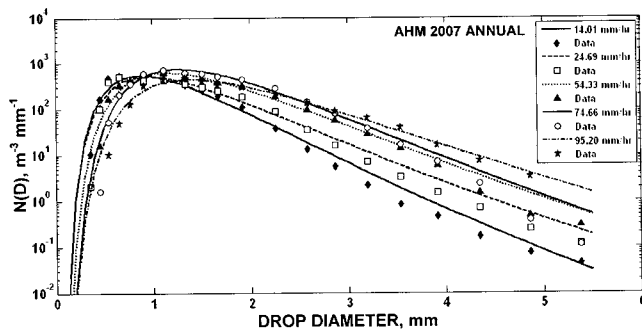


Fig. 5 — Annual rain drop size distribution spectrum 2007

4.4.1 Comparison of fit parameters with other models

The values of the fit parameters A, B and C have been compared, at different rain rates, with those reported by Hari Kumar *et al.*¹⁴ by histograms in Fig. 8. Models reported in ref. 14 are based on disdrometer data collected at Thiruvananthapuram, Kochi, Munnar and Sriharikota which are coastal areas of India. There is not much difference in the value of parameter A but there is considerable variation in parameter B. Parameter B basically represents geometric mean of drop diameter and its value is high in case of model developed in ref. 14. From this comparison, an inference can be

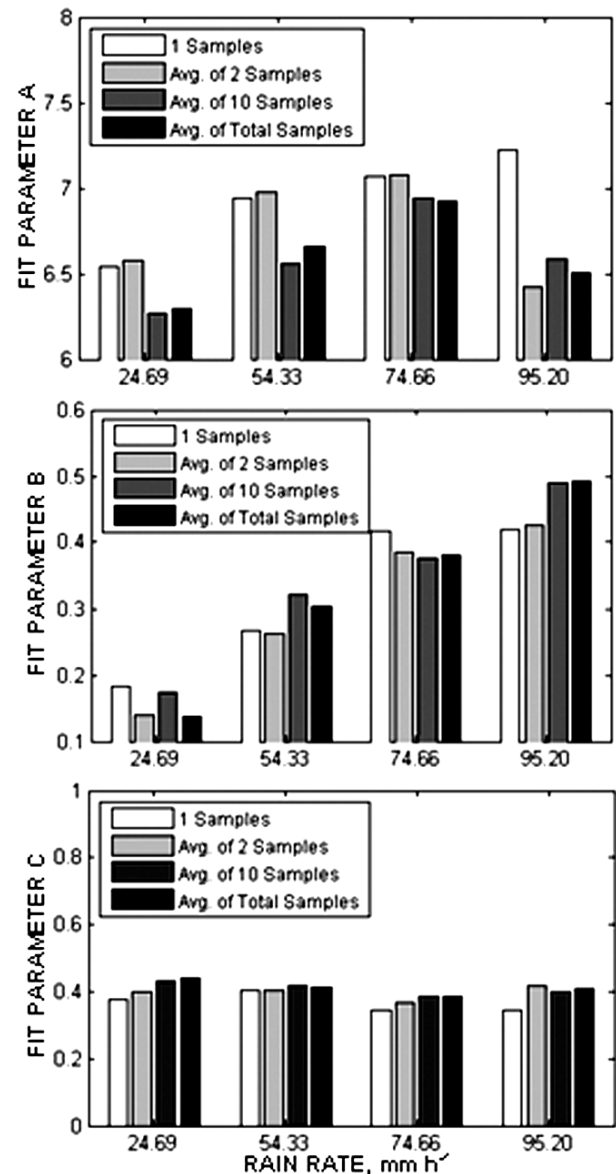


Fig. 6 — Variation of fit parameter A, B and C with number of rain samples

drawn that there is more concentration of the drops with larger diameter in case of coastal rains compared to the rains in plan area like Ahmedabad. This fact is very important from the attenuation point of view at millimeter wave frequencies. This gives strength to the philosophy of data collection, on DSD, at various places representing different meteorological conditions within India. The parameter C which represents standard deviation of drop sizes is almost same at 0.4 in both the cases. From the above discussion, it can be inferred that the drop size distribution cannot be generalized and depends on the type of rain. In the coastal areas, the rain characteristics are different from those observed at Ahmedabad. Similar analysis has also been reported by Fang & Chen²² and Ajayi

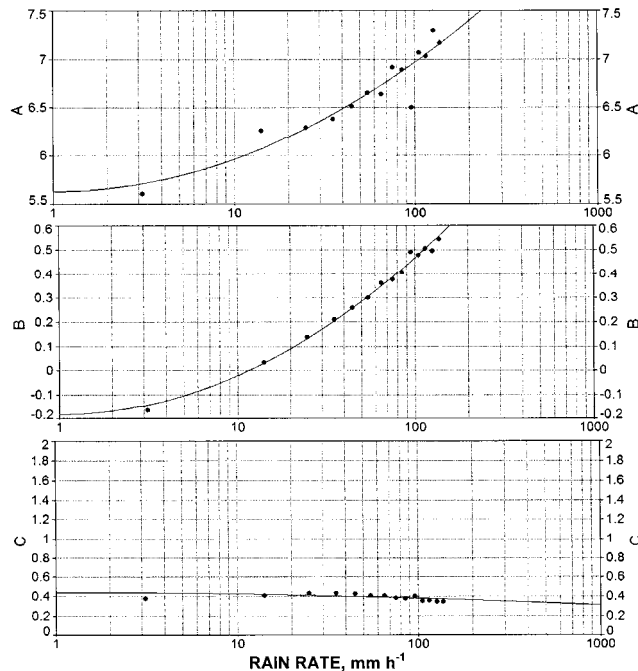


Fig. 7 — Variation of the fit parameter A, B and C with rain rate

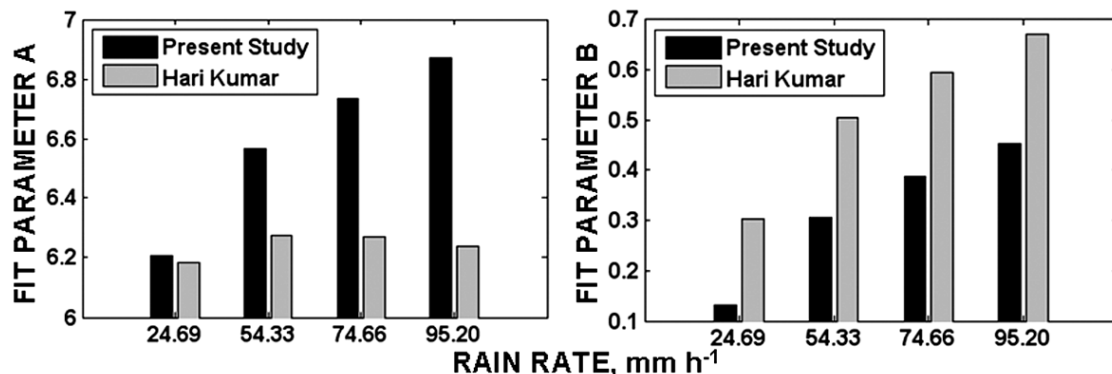


Fig. 8 — Comparison of modeled fit parameters A and B with others

& Olsen²³ for data collected in temperate climate and Nigeria. The values of fit parameters, for lognormal distribution, reported therein are at variance when compared with those for India presented in present work and given by Hari Kumar *et al.* in ref. 14.

5 Validation of Empirical model

To validate the annual empirical model, the experimental data points, at average rain rate corresponding to all the fourteen rain rate bins have been plotted over the model derived curves in Fig. 9 using A, B and C values obtained from Eqs (11-13). Curves derived from model reported in ref. 14 are also plotted therein for comparison. The correlation coefficients, between model derived and experimental values of $N(D)$, have been plotted in Fig. 10 at each rain rate. The values of correlation coefficients have been found to lie between 0.932 and 0.994 which shows very good correlation between the model and the experimental data. It can be seen from Fig. 9 that for the rain rates upto 74.66 mm h^{-1} , no drop has fallen in the last disdrometer bin corresponding to diameter 5.5 mm . At rain rates 84.29 and 95.20 mm h^{-1} , drops have been recorded in the 5.5 mm diameter bin and the number of drops recorded is more than the drops recorded in the next lower bin corresponding to 4.86 mm diameter which is against the normal trend observed in lower diameter bins. The possible reason for this may be the presence of the drops with diameter larger than 5.37 mm (the drops recorded in the bin with 5.35 diameter have also been considered in the development of empirical model). The reason for the absence of drops in the last bin at rain rates 104.40 mm h^{-1} and higher may be due to splitting

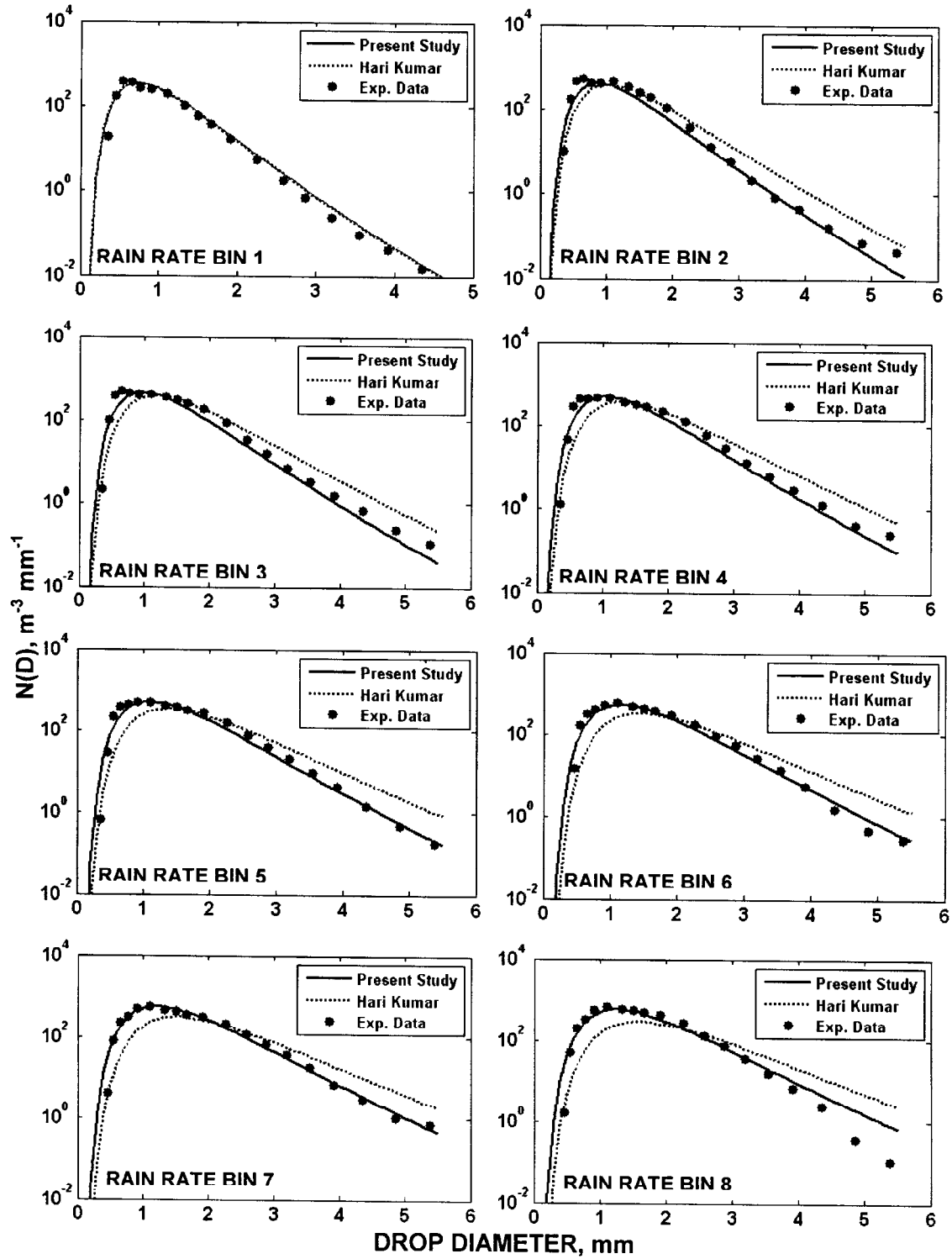


Fig. 9 — Validation of empirical model developed with experimental data and comparison with model developed by Hari Kumar

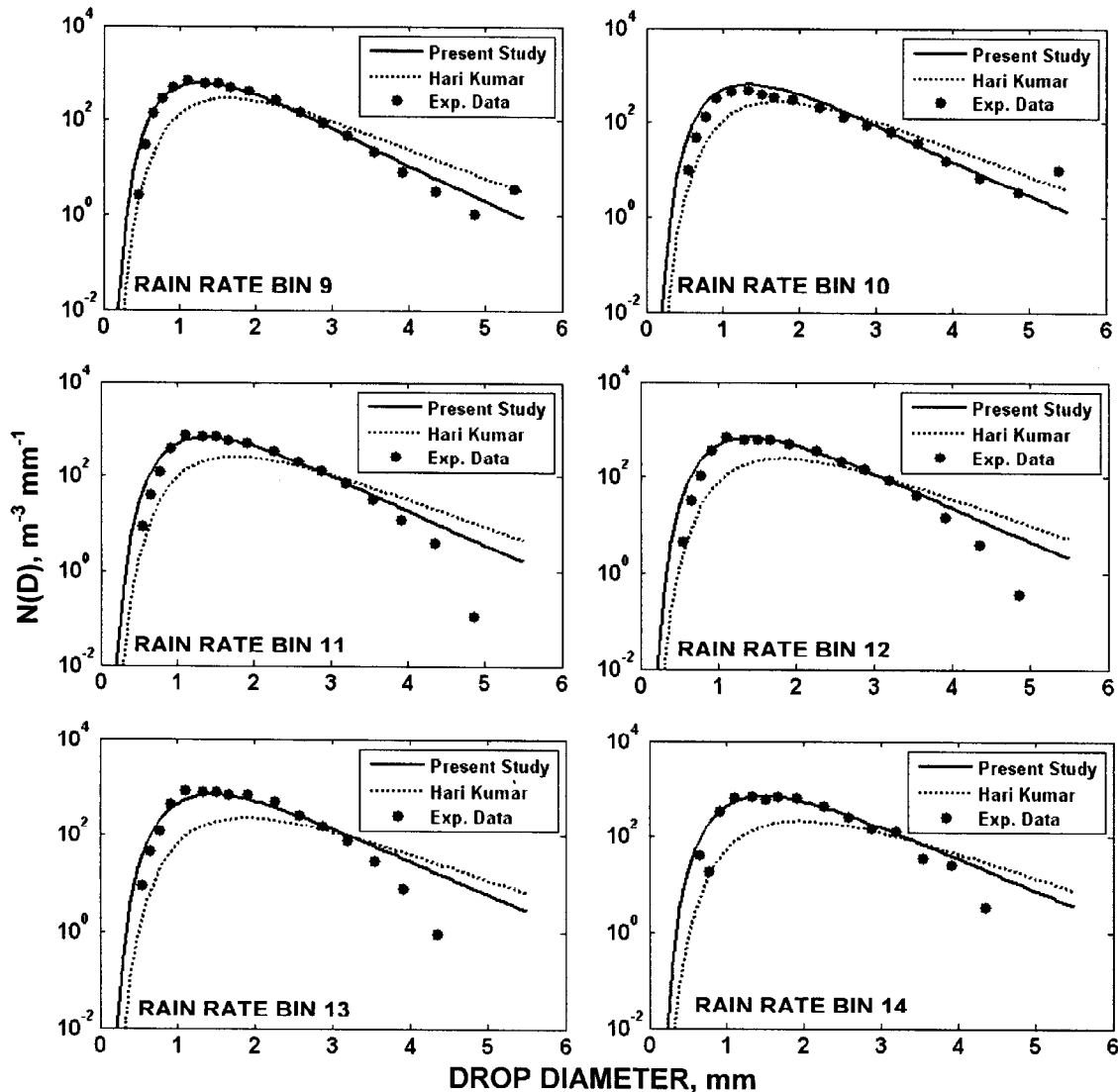


Fig. 9 (Contd.)—Validation of empirical model developed with experimental data and comparison with model developed by Hari Kumar

of larger drops into smaller drops at higher rain rates. The other possible reason could be the change over from stratiform rain to convective rain at which the number of smaller drops is reported to be higher and the number of larger drops is less¹⁹. The number of rain events, of 30 seconds each, recorded at 104, 114, 125 and 136 mm h⁻¹ were 26, 21, 8 and 1, respectively. It has been generally observed that the rains above 100 mm h⁻¹ are isolated events and do not represent the normal monsoon rains falling from June to September. For a communication engineer, rain rates exceeding 0.01% of the time, on long term basis (an year or more), is of interest which

in the present case happens to be 74.66 mm h⁻¹ on yearly basis.

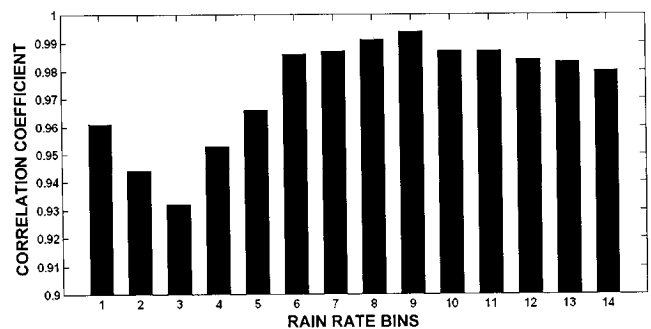


Fig. 10 — Correlation coefficients between modeled and experimental DSD for different rain rate bins

6 Conclusions

Drop size distribution model is developed for a tropical site Ahmedabad, India. Good correlation obtained between the experimental results and model, authenticates the finding reported by other researchers that the lognormal distribution is more suitable for tropical regions. However, from the present study, it is evident that the values of fit parameters differ from place to place as found for Ahmedabad in present study and reported by others for coastal areas of India. Moreover, rate of rainfall (mm h^{-1}) and duration also depends on the climatic conditions. Similar study should also be carried out for central and northern regions of India. Such data is essential for designing the reliable millimeter wave communication links, meeting the desired percentage reliability criterion, for different meteorological regions of the country.

Acknowledgements

The authors are thankful to Indian Space Research Organization (ISRO), Bangalore and Space Application Centre (SAC), Ahmedabad for providing the raw data and financial support for the project activity.

References

- Crane Robert K, *Electromagnetic wave propagation through rain* (John Wiley, New York), 1996.
- Davarian Farmaz, *An update on NASA Ka-band propagation measurements* (Jet Propulsion Lab, California), 1994, 91109.
- Hari Kumar R, Sasi Kumar V, Sampath S & Vinayak P V S S K, Comparison of drop size distribution between stations in Eastern and Western coasts of India, *J Indian Geophys Union*, 11 (2) (2007) pp 111-116.
- Kozu T, Reddy K K, Mori S, Thurai M, Ong J T, Rao D N & Shimomai Toyoshi, Seasonal and diurnal variations of raindrop size distribution, *J Meteorol Soc Jpn (Japan)*, 84A (2006) pp 195-209.
- Lakshmi S K, Lee Y H & Ong J T, Truncated gamma drop size distribution models for rain attenuation in Singapore, *IEEE Trans Antennas Propag (USA)*, 58 (4) (2010) pp 1325-1335.
- Ajayi G O & Olsen R L, Measurement and analysis of rain drop size distribution in South Western Nigeria, *Proceeding International Radio Science Union, Commission For Symposium on Wave Propagation and Remote Sensing, ESA SP-194* (Louvain, Belgium), 1983, pp 173-184.
- Marshall J S & Palmer W M, The distribution of raindrops with size, *J Atmos Sci (USA)*, 5 (1948) pp 165-166.
- Joss J & Waldvogel A, Ein spektrograph fur neiderschlagestrophen mit automatischer auswertung, *Pure Appl Geophys (Switzerland)*, 68 (1967) pp 240-246.
- Joss J & Gori E, Shapes of rain size distributions, *J Appl Meteorol (USA)*, 17 (1978) 1054.
- Takeuchi D M, Characterization of raindrop size distributions, *Conf on Cloud Physics and atmospheric Electricity, Issaquah* (Am Meteorol Soc, Boston), 1978, pp 154-161.
- Ulbrich C W, Natural variations in the analytical form of the rain drop size distribution, *J Clim Appl Meteorol (USA)*, 22 (1983) pp 1764-1775.
- Willis P T & Tattelman P, Drop-size distribution associated with intense rainfall, *J Appl Meteorol (USA)*, 28 (1989) pp 3-15.
- Feingold G & Levin Z, The lognormal fit to raindrop spectra from frontal convective clouds in Israel, *J Clim Appl Meteorol (USA)*, 25 (1986) pp 1346-1363.
- Harikumar R, Sampath S & Sasi Kumar V, An empirical model for the variation of rain drop size distribution with rain rate at a few locations in southern India, *Adv Space Res (UK)*, 43 (2009) pp 837-844.
- Sauvageot H & Lacaux J P, The shape of averaged drop size distributions, *J Atmos Sci (USA)*, 52 (1995) pp 1070-1083.
- Das S, Mitra A & Shukla A K, Rain attenuation modeling in the 10-100 GHz frequency using drop size distributions for different climatic zones in tropical India, *Prog Electromagn Res (Hong Kong)*, 25 B (2010) pp 211-224.
- Odedina M O & Afullo T J, *Analytical modeling of rain attenuation and its application to terrestrial LOS links*, Southern Africa Telecommunication Networks and Application Conference (SATNAC) (Royal Swazi Spa, Swaziland), 2009.
- Gunn R & Kinzer G D, The terminal velocity of fall for water droplets in stagnant air, *J Atmos Sci (USA)*, 6 (4) (1949) pp 243-248.
- Tokay A & Short D A, Evidence from tropical raindrop spectra of the origin of rain from stratiform versus convective clouds, *J Appl Meteorol (USA)*, 35 (1996) pp 355-371.
- Shukla A K, Roy B, Das S, Charania A R, Kavaiya K S, Bandyopadhyay K & Dasgupta K S, Micro rain cell measurements in tropical India for site diversity fade mitigation estimation, *Radio Sci (USA)*, 45 (2010) RS1002.
- Jassal B S, Verma A K & Lal Singh, Rain drop-size distribution and attenuation for Indian climate, *Indian J Radio Space Phys*, 23 (3) (1994) pp 193-196.
- Fang D J & Chen C H, Propagation of centimeter/millimeter waves along a slant path through precipitation, *Radio Sci (USA)*, 17 (5) (1982) pp 989-1005.
- Ajayi G O & Olsen R L, Modeling of a tropical raindrop size distribution for microwave and millimeter wave applications, *Radio Sci (USA)*, 20 (2) (1985) pp 193-202.